

Brain location and visual topography of cortical area V6A in the macaque monkey

Claudio Galletti, Patrizia Fattori, Dieter F. Kutz¹ and Michela Gamberini

Dipartimento di Fisiologia umana e generale, Università di Bologna, Piazza di Porta S. Donato 2, 40127, Bologna, Italy

¹Department of Zoology and Neurobiology, Ruhr-University Bochum, D-44780 Bochum, Germany

Keywords: prestriate cortex, reaching, superior parietal lobule, visuomotor integration

Abstract

The brain location, extent and functional organization of the cortical visual area V6A was investigated in macaque monkeys by using single cell recording techniques in awake, behaving animals. Six hemispheres of four animals were studied. Area V6A occupies a horseshoe-like region of cortex in the caudalmost part of the superior parietal lobule. It extends from the medial surface of the brain, through the anterior bank of the parieto-occipital sulcus, up to the most lateral part of the fundus of the same sulcus. Area V6A borders on areas V6 ventrally, PEc dorsally, PGM medially and MIP laterally. Of 1348 neurons recorded in V6A, 61% were visual and 39% non-visual in nature. The visual neurons were particularly sensitive to orientation and direction of movement of visual stimuli. The inferior contralateral quadrant was the most represented one. Visual receptive fields were also found in the inferior ipsilateral quadrant and in the upper visual field. Receptive fields were on average smaller in the lower visual field than in the upper one. Both central and peripheral parts of the visual field were represented. Large parts of the visual field were represented in small regions of area V6A, and the same regions of the visual field were re-represented many times in different parts of this area, without any apparent topographical order. The only reliable sign of retinotopic organization was the predominance of central representation dorsally and far periphery ventrally. The functional organization of area V6A is discussed in the view that this area could be involved in the control of reaching out and grasping objects.

Introduction

For a long time, the monkey superior parietal lobule (SPL) has been thought to be involved in the analysis of somatic signals and somatomotor activity, both related to the movement of the arm, without any role in visual or visuomotor processing (see Stein, 1991). Yet, it was known since the beginning of this century that SPL contained also a visual region. Brodmann (1909) reported the presence of the most medial part of area 19, a cortical visual association area, in the caudalmost part of SPL. Later on, von Bonin & Bailey (1947) confirmed this view reporting that the cortex of the anterior bank of the parieto-occipital sulcus (APO) was occupied by the most medial part of what they called area OA, the homologous of Brodmann's area 19.

More recently, extracellular recordings in anaesthetized and paralysed animals confirmed the visual nature of this same brain region: a visual area, named PO, was located in the ventral part of APO (Colby *et al.*, 1988). PO neurons were described as very sensitive to visual stimulations and retinotopically organized. The same authors reported the presence of visual neurons also in the cortex dorsal to PO, although these cells were described as less responsive to visual stimulation with respect to the neurons of area PO.

Recent recordings from single neurons in awake animals have confirmed that in APO at least two cortical visual areas are present: area V6 (PO) ventrally and area V6A dorsally (Galletti *et al.*, 1996). According to this study, both areas contain visual neurons that, when correctly activated, produce high firing rates of discharge. Some V6A

visual neurons are also able to encode directly the spatial coordinates of visual objects, as their receptive field remains anchored to the same spatial location irrespective of the direction of gaze (Galletti *et al.*, 1993). While all neurons of area V6 are visual in nature, area V6A contains visual neurons as well as neurons insensitive to visual stimulation. The activity of V6A non-visual neurons is modulated by oculomotor activities, such as fixations towards particular regions of visual space or changes in the direction of gaze (Galletti *et al.*, 1991, 1995), and/or by somatomotor activities, in particular by the movement of the arms (Galletti *et al.*, 1997a). In summary, area V6A seems to have a complete machinery to allow orienting of the animal towards objects present in the visual field, and to visually guide the reaching movements toward those same objects.

The aim of this work is to describe the brain location and extent of area V6A, and to study the visual topography of this area in order to discuss its functional organization with respect to the suggested role in visuomotor processing. Preliminary data on this matter have been previously published in abstract form (Galletti *et al.*, 1997b).

Materials and methods

Four monkeys (*Macaca fascicularis*; 3.1–7.1 kg) were used in this study. Experimental protocols were approved by the Bioethical Committee of the University of Bologna and were in compliance with the national and European laws on the care and use of laboratory animals. A detailed description of training, anaesthetic, surgical and recording procedures, as well as of visual stimulation, anatomical reconstruction of recording sites and animal care are reported else-

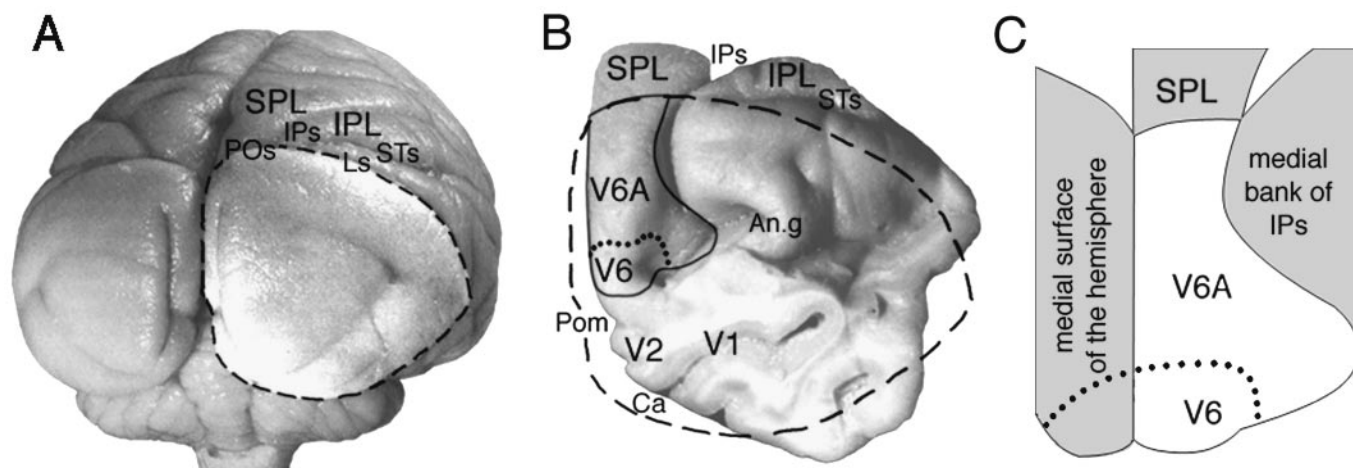


FIG. 1. Brain location of area V6A. (A) Posterior view of macaque brain (*Macaca fascicularis*). The right occipital pole is shown lightened and bordered by a dashed line. SPL: superior parietal lobule; IPL: inferior parietal lobule; IPs: intraparietal sulcus; Ls: lunate sulcus; POs: parieto-occipital sulcus; STs: superior temporal sulcus. (B) Posterior view of the right hemisphere of macaque brain after occipital pole dissection. The occipital pole has been cut away (dashed line) to show the anterior banks of POs medially and of Ls laterally. The anterior bank of POs has been bordered by a continuous line. A dotted line indicates the border between areas V6 and V6A. An.g: angular gyrus; Ca: calcarine fissure; Pom: medial parieto-occipital sulcus; V1, V2, V6, V6A: areas V1, V2, V6 and V6A. Other abbreviations as in A. (C) Two-dimensional map of the caudal pole of SPL. The cortical mantle has been cut along the curvatures between the medial surface of the hemisphere and the dorsal surface of SPL, and between this latter and the medial bank of IPs. These three brain surfaces are shown in grey and on the same plane of the anterior bank of POs (shown in white). A dotted line indicates the border between areas V6 and V6A as in B.

where (Galletti *et al.*, 1995). The following is a brief description of them.

Before surgery, the animals were sedated with ketamine hydrochloride (12 mg/kg i.m.). All surgical procedures were performed under aseptic conditions using sodium thiopental i.v. (15 mg/kg initially followed by 8 mg/kg/h). The animals received analgesics for 2 days and were given free access to water fruit and chow for \approx 2 weeks. Animals performed fixation tasks with the head restrained while single neurons from the cortex of the posterior pole of SPL were extracellularly recorded by home-made glass-coated Elgiloy microelectrodes (Suzuki & Azuma, 1976). During recording sessions, animals sat in a primate chair facing a large ($80^\circ \times 80^\circ$) tangent screen. They were trained to look at a fixation spot projected on the screen for 2–6 s without reacting to any other visual stimulus present on the same screen during this period. Eye positions were recorded by an infra-red oculometer (Dr Bouis, Germany; Bach *et al.*, 1983). The sample rate for action potentials was 1 kHz and that for eye position 100 Hz.

A standard protocol was used for testing the visual responsiveness of cells in record. Cells were first tested with simple visual stimuli (light/dark borders, light or dark bars and spots of different size, orientation, direction and speed of movement) rear-projected on the screen facing the animal. If the neuron in record was not responsive to these stimuli, testing was continued using more complex visual stimulations (light/dark gratings and corners of different orientation, direction and speed of movement). In some cases, cells that were at first responsive to complex visual stimuli then rapidly adapted to the continued visual stimulation, becoming unresponsive to it (see Galletti *et al.*, 1996). This type of cell remained active only if the visual stimuli delivered on their receptive fields were continuously changed in orientation, direction and/or speed of movement.

As the visual responsivity of many V6A cells was strongly modulated by the direction of gaze (Galletti *et al.*, 1995), the possibility existed that a cell was not responsive to visual stimulation because the animal was looking towards a non-preferred direction. For this reason, simple and complex visual stimulations were repeated while the animal gazed at different screen locations. This procedure

also allowed us to check whether the visual receptive field was organized in retinotopic or craniotopic coordinates.

In cases where we were not able to activate the cell in record with the battery of simple and complex visual stimuli above described, we classified that cell as non-visual in nature. If the cell was visually responsive, on the contrary, we mapped the borders of visual receptive field with the optimal stimulus, chosen among the battery we had tested.

At the end of recording sessions, the animals were killed with an overdose of i.v. thiopental. Electrode tracks and the approximate location of each recording site were reconstructed on parasagittal sections of the brain on the basis of marking lesions and several other cues, such as the coordinates of penetrations within recording chamber, the kind of cortical areas passed through before reaching the APO, the location of boundaries between white and grey matter, and the distance of recording site from the surface of the hemisphere.

Two-dimensional reconstruction of recording sites

Figure 1 shows the cortex of the posterior pole of SPL, where recordings have been carried out, together with a two-dimensional (2D) map of this same cortical region. The partial unfolding method of Van Essen & Zeki (1978) was used to construct the 2D map from parasagittal sections of the brain. The construction of the map depended on two fixed points of reference in the brain. One was the dividing line between the APO and the medial surface of the hemisphere. The other was the crown of SPL, i.e. the dividing line between the cortex in the APO and that in the dorsal surface of the hemisphere. To afford comparability between different cases these two reference lines adopted the same position in all our 2D reconstructions. Elsewhere the forms of the contours were free to reflect the variable gyral morphology of each case. Note that the APO, shown outlined in Fig. 1B and in white in Fig. 1C, is not a straight wall in a coronal plane, as it could be supposed by looking at the course of the parieto-occipital sulcus in a dorsal view of the brain. Actually, the APO is bent anteriorly from medial to lateral, particularly in its ventrolateral part, as can be seen in Fig. 1B as well as in any horizontal section of the brain passing near the fundus of the parieto-occipital sulcus.

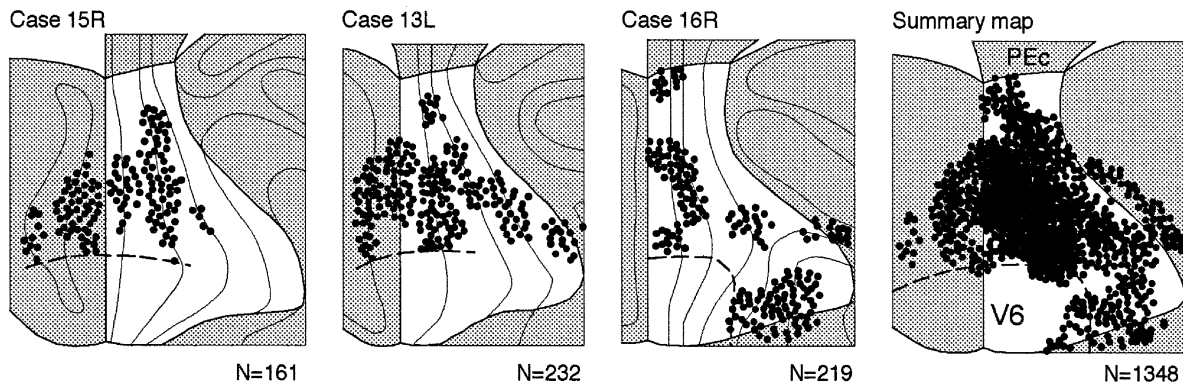


FIG. 2. Recording sites in V6A. Two-dimensional maps of the caudal pole of SPL in three different cases, and in a summary case that contains all V6A cells recorded from six hemispheres. Filled circles within the maps indicate brain locations of recorded cells attributed to area V6A on the basis of functional criteria described in Galletti *et al.* (1996). The total number of recorded cells is reported at the bottom of each map. Dashed lines indicate location of the border between areas V6 and V6A as determined by functional characteristics of recorded cells (see Galletti *et al.*, 1996). In the summary map, dashed line indicates the average location of V6/V6A border in six hemispheres. PEc and V6: areas PEc and V6. Details on 2D maps as in Fig. 1.

As shown in Fig. 1C, we introduced two discontinuities in the 2D map between neighbouring cortical surfaces. They were at points of maximum local curvature of the cortical mantle: medially, between the dorsal and medial surfaces of the hemisphere, and laterally, between the dorsal surface of the hemisphere and the medial bank of intraparietal sulcus (IPs).

Each recording site was marked on a 2D map according to our best estimate of the location of the electrode track and of the cell along the track. The map and recording sites were digitized, and linked by purpose-written software to the database storing the functional properties of each unit, enabling rapid analysis of the distribution of any given functional characteristic. In some cases, the maps of different animals were combined to give an overall summary diagram of the data. To do this, the maps of different cases were aligned according to the two reference lines described above. As we decided to show summary data on the right hemisphere, the maps derived from left hemispheres were reflected. Before superimposition, each map was rescaled according to the relative size of the whole brain and the dorsoventral extent of APO. The maximum rescaling factor used was 9%.

Results

Microelectrode penetrations were carried out in six hemispheres of four animals. Cells were recorded from the posterior part of the SPL, involving four cortical surfaces: the medial and dorsal surfaces of the SPL, the medial bank of IPs and the APO (see Fig. 1C). All cells recorded from the dorsal surface of SPL turned out to be not activated by visual stimulation and were assigned to area PEc (Pandya & Seltzer, 1982). The other recorded cells were either visual or non-visual in nature. Penetrations with mixed visual/non-visual cells were assigned to area V6A, according to Galletti *et al.* (1996). Penetrations with only visual neurons were assigned to areas V6 or V6A on the basis of the functional criteria illustrated below and in Galletti *et al.* (1996), as well as on the basis of the sequence of receptive-field locations observed along the penetration (see below).

Figure 2 shows the cortical distribution of V6A cells recorded in three different hemispheres, and a summary map with the locations of all V6A cells recorded in the six hemispheres we studied. This summary map roughly indicates the extent and limits of area V6A. It occupies a horseshoe-like region of cortex extending from the medial surface up to the dorsal and ventrolateral parts of the APO. Area V6A borders on

areas PEc dorsally and V6 ventrally. The location of its medial and lateral borders are more uncertain (see Discussion).

Area V6A contains two types of neurons: sensitive and insensitive to visual stimulation. Those classified as insensitive to visual stimulation were neurons neither activated by simple stimuli (light/dark borders, light or dark bars and spots of different size, orientation, direction and speed of movement), nor by more complex visual stimuli (light/dark gratings and corners of different orientation, direction and speed of movement) projected on the screen facing the animal. Of 1348 neurons recorded from 132 microelectrode penetrations in V6A, 827 (61%) were visual and 521 (39%) non-visual in nature. These two types of neurons were not spatially segregated within area V6A (see also Galletti *et al.*, 1996). In single penetrations, the two types of cells could be encountered in groups or isolated without any apparent rule. We also checked the possibility that visual and non-visual neurons were differentially distributed according to the distance of recording site from the cortical surface, but we were not able to demonstrate such a type of correlation. In summary, it seems a peculiarity of area V6A to have both types of cells mixed together. This peculiarity clearly distinguishes area V6A from both area V6, whose neurons are all sensitive to visual stimulation (Galletti *et al.*, 1996), and area PEc, whose neurons are all insensitive to visual stimulation (C. Galletti, unpublished observations).

The receptive-field size of V6A visual neurons increased with eccentricity, as is usual in any cortical visual area. Figure 3A shows the plot of receptive-field size (square root of area) against receptive-field eccentricity in a population of V6A visual cells recorded from all the six hemispheres we studied. Data are highly scattered, meaning that small as well as large receptive fields can be found at any value of eccentricity. Figure 3B shows that, on average, the size of receptive-fields whose centre was located in the upper visual field was larger than that in the lower one (ANCOVA, $P < 0.0001$). Note that the high scattering of data generates low levels of correlation in all V6A cell populations, but the upper and lower visual-field regression lines show better determination coefficients with respect to that of the whole V6A population ($r^2 = 0.33$ and 0.22 with respect to 0.15).

Figure 4 shows the retinotopic distribution of receptive-field centres of the same group of cells reported in Fig. 3, together with the outline of the most peripheral receptive-field borders. It is evident that both central and peripheral (up to about 80°) parts of the visual field are represented in V6A. Although the contralateral inferior quadrant is the most represented one, receptive fields were also found in the ipsilateral inferior quadrant and in the upper visual field.

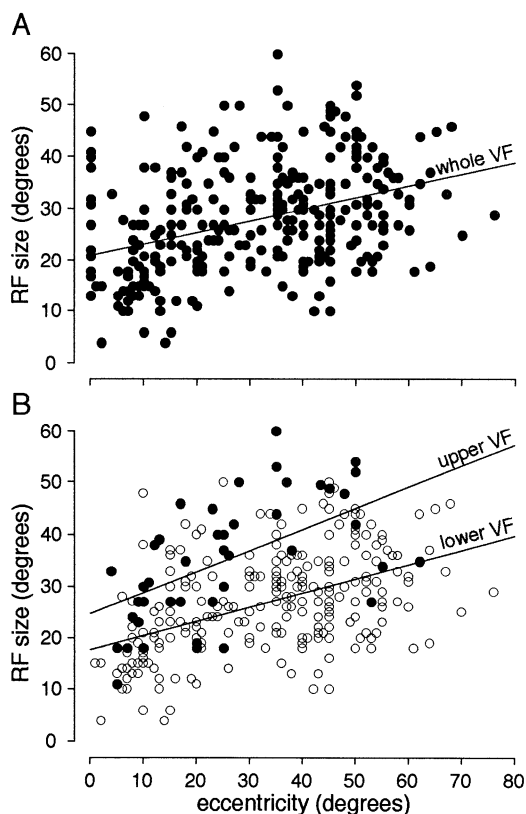


FIG. 3. Receptive-field size vs. eccentricity in area V6A. (A) Regression plot of receptive-field size (square root of area) against eccentricity for 410 visual cells recorded in V6A. The regression equation is:

$$\text{size} = 21.0^\circ + 0.22\text{ecc}; r^2 = 0.15$$

(B) Dual regression plot of receptive-field size against eccentricity for V6A visual cells with receptive field in the upper (filled circles) and lower (empty circles) visual field (VF), respectively. Cells with receptive field at 0° of eccentricity ($N = 21$) have been discarded from this analysis. The regression equations are:

$$\text{Upper VF (N = 49): size} = 24.6^\circ + 0.41\text{ecc}; r^2 = 0.33$$

$$\text{Lower VF (N = 340): size} = 17.6^\circ + 0.28\text{ecc}; r^2 = 0.22$$

ANCOVA analysis established that the two regression lines were not significantly different in slope ($F_{1,385} = 2.52$; $P = 0.1$) but they were significantly different in elevation (mean difference in receptive field size = 10.5° ; $F_{1,386} = 60.5$; $P < 0.0001$).

About 10% (28 of 290) of V6A visual neurons had receptive fields not organized in retinotopic coordinates, as on the contrary is usual for visual neurons in the visual system. The receptive field of this type of cell remained anchored to the same spatial location irrespective of eye movements. These neurons were not included in the cell population of Figs 3 and 4 because their receptive fields showed retinotopic coordinates that were not constant: they changed according to the changes of gaze direction. A detailed description of these so-called *real-position cells* has been reported in a previous publication (Galletti et al., 1993). Figure 5 shows the distribution of real-position cells on a summary map of the caudal pole of SPL. Real-position cells were found only in area V6A, mainly in its ventral part. No real-position cells were found within the limits of area V6.

Visual topography in area V6A

In order to study the visual topography in area V6A, we reconstructed all microelectrode penetrations of the six hemispheres we studied on parasagittal sections of the brain, and analysed the sequence of recep-

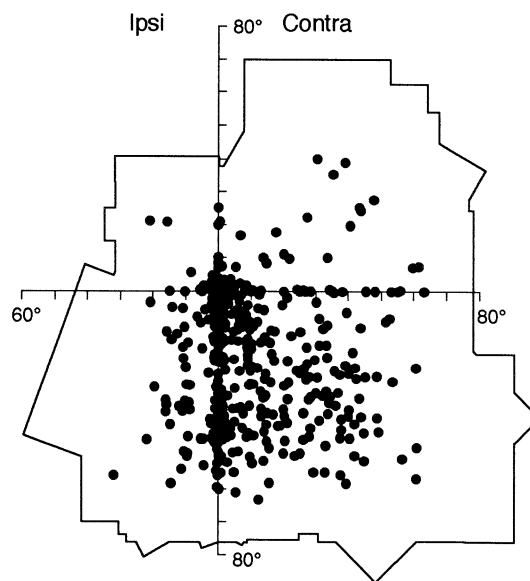


FIG. 4. Visual field representation in V6A. Filled circles indicate the retinotopic distribution of receptive-field centres of the same cell population shown in Fig. 3. An outline of the most peripheral receptive-field borders is also reported.

ive-field locations along each penetration. Figure 6 is an example of this work. Eight penetrations have been reconstructed on two parasagittal brain sections of case 16R. Five penetrations are reported on section A, three that reach area V6A in the dorsal part of APO (penetrations a, b, c), and two reaching area V6 in the deepest part of APO (d, e). Looking at the sequences of receptive-field locations shown in the insets of the figure, it is evident the different behaviour in the two cortical areas. In area V6, successive receptive fields encountered along each penetration showed a small, 'physiological' scattering: they remained more or less in the same spatial location, or moved away jerkily but in small steps and, on average, towards the same direction. In contrast, a large scattering of receptive fields was usually observed in area V6A. Receptive fields in this area could remain in the same spatial location

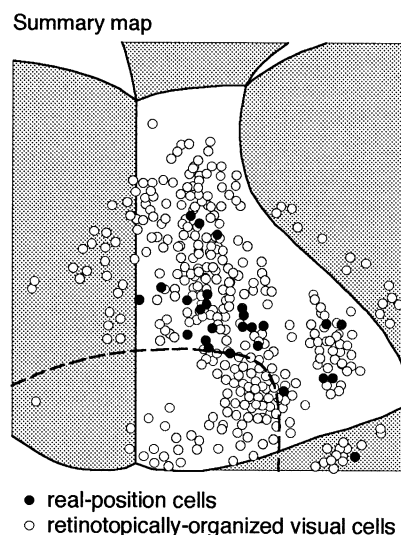


FIG. 5. Real-position cell distribution in the caudal SPL. Circles on the 2D map of the caudal pole of SPL indicate locations of cells tested for real-position behaviour. Filled symbols are locations of real-position cells, empty symbols of retinotopically organized visual cells. Data are derived from six hemispheres. Dashed line indicates the average location in the six hemispheres of the border between areas V6 and V6A. Details on 2D map as in Fig. 1.

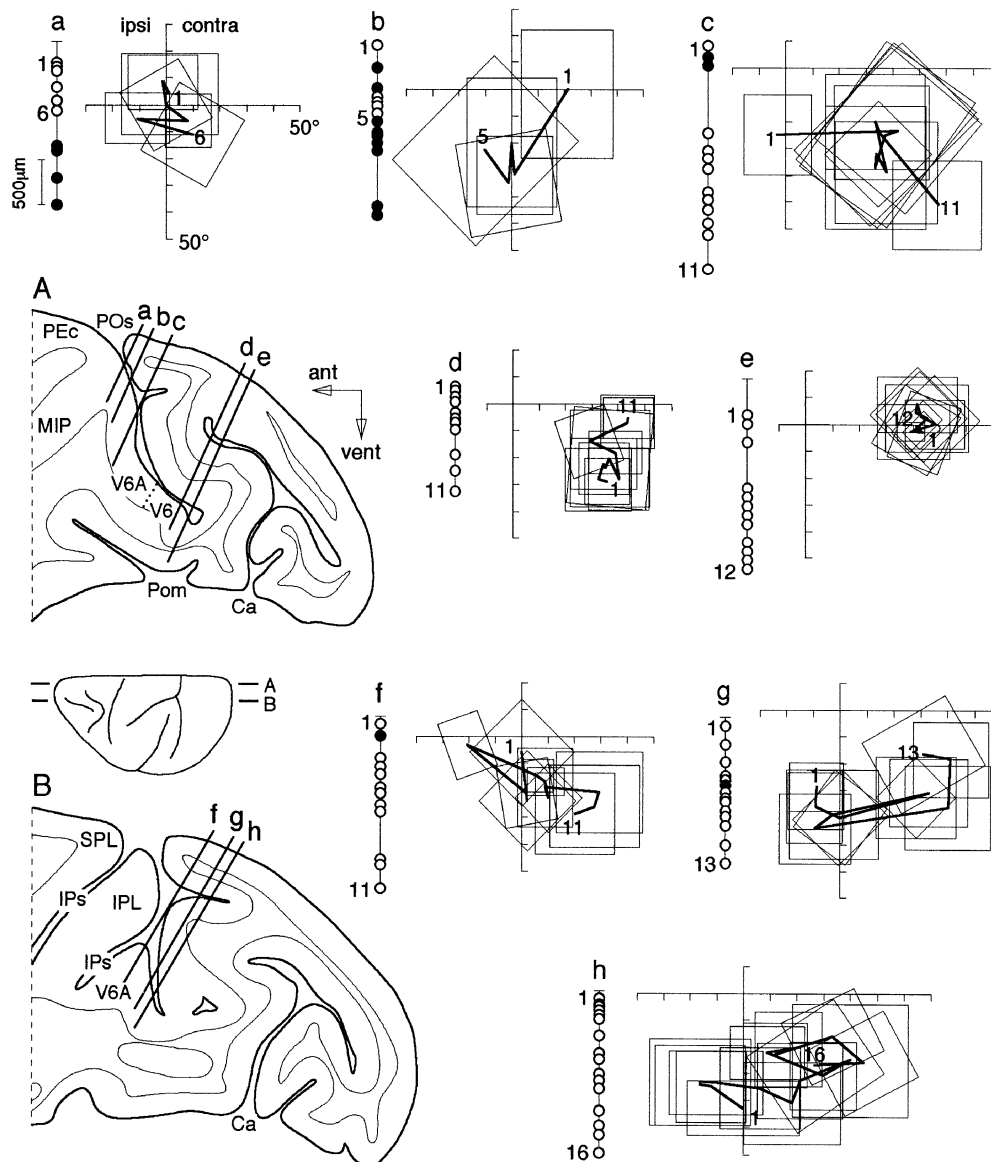


FIG. 6. Visual receptive fields plotted in penetrations made through areas V6A and V6. A and B, on the left, are two parasagittal sections of the brain of case 16R, taken at the levels shown on brain silhouette. Eight reconstructed penetrations are shown on the two sections. Six penetrations (a–c, f–h) reached area V6A, two (d,e) area V6. One inset for each penetration is shown on the top and right part of the figure. Each of the eight insets shows the cell types encountered and their locations along the penetration (empty circles = visual cells; filled circles = non-visual cells), and the receptive-field sequence of visual neurons. Visual cells are numbered progressively along the penetration track: first and last numbers are reported. The receptive-field centres of visual cells are sequentially connected with a thick line. First and last field encountered in the penetration are numbered. SPL: superior parietal lobule; IPL: inferior parietal lobule; IPs: intraparietal sulcus; Ca: calcarine fissure; Pom: medial parieto-occipital sulcus; POCs: parieto-occipital sulcus; ant: anterior; vent: ventral; POC, MIP, V6A, V6: areas POC, MIP, V6A, V6.

for hundreds of microns, and then jump away in an unpredictable direction. In other words, cells near one to another in V6A could have receptive fields either in the same or in completely different locations in the visual field. Receptive-field jumping in V6A and physiological scattering in V6 were phenomena constantly seen in all cases we studied.

In section B of Fig. 6 the reconstruction of three other penetrations (f, g, h) is reported. They reached area V6A in the ventral part of APO, some millimetres laterally with respect to section A. Again, receptive-field jumps are clearly evident. The receptive fields jumped from central to peripheral locations, or from ipsilateral to contralateral parts of the visual field. In other cases, not shown in the figure, they jumped from lower to upper parts of the visual field as well. In many penetrations, as in some of those shown in Fig. 6, receptive fields jumped repeatedly forward and backward, in completely different sectors of the visual field.

The existence of receptive-field jumping with unpredictable directions all over V6A means that in this area the visual field is not represented in an orderly way. It seems therefore a nonsense to talk about visual topography in area V6A. However, it might be that large sectors of the visual field, such as a quadrant or an hemifield, were *predominantly* represented in different parts of the SPL. To check this possibility, we analysed the distribution of receptive-field locations on the 2D maps of single cases.

The upper part of Fig. 7 shows an example of this study. As predicted by the previous analysis of receptive-field sequence in single penetrations, data on 2D maps of single cases confirmed that different parts of the visual field are represented in the same region of V6A, and that the same part of visual field is re-represented in different parts of V6A. In the summary map of the lower part of Fig. 7 data from six hemispheres

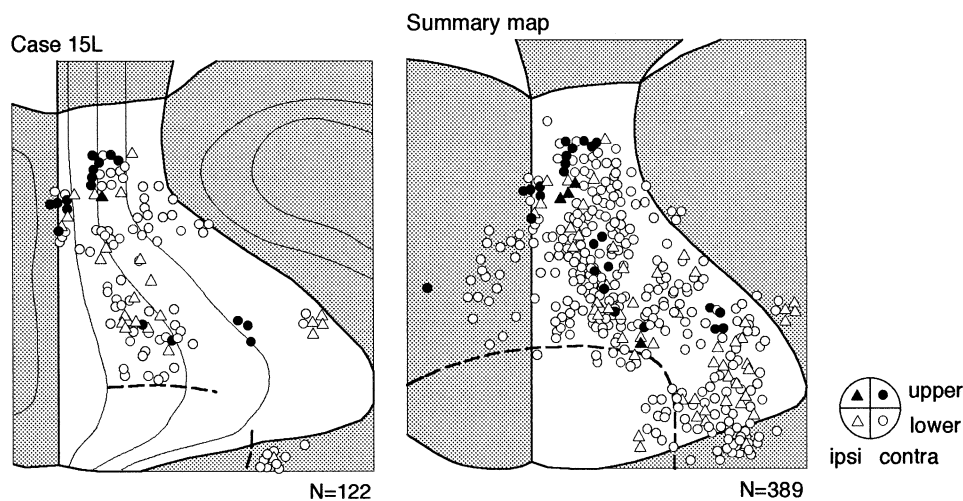


FIG. 7. Visual topography in V6A: quadrant representation. The 2D map of the caudal pole of SPL in case 15L and in a summary case are shown. The summary case shows data from six hemispheres. Different symbols (filled and empty circles and triangles) indicate map locations of V6A cells whose receptive-field centres were in different parts of the visual field. As indicated at the bottom left of the figure, black (filled symbols) indicate receptive-field centres in the upper part of the visual field, white (empty symbols) in the lower part, triangles in the ipsi and circles in the contralateral parts. Details on 2D map as in Fig. 1.

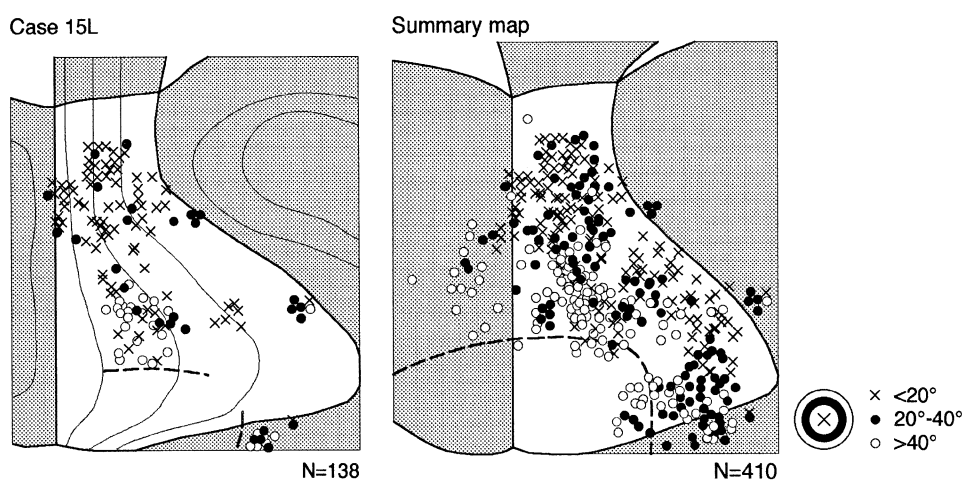


FIG. 8. Visual topography in V6A: eccentricity representation. The 2D map of the caudal pole of SPL in case 15L and in a summary case are shown. The summary case shows data from six hemispheres. Different symbols (crosses, filled and empty circles) indicate map locations of V6A cells whose receptive-field centres had different eccentricities. As reported at the bottom left of the figure, crosses indicate receptive-field centres within the central 20° , filled circles between 20° and 40° , and empty circles receptive fields more eccentric than 40° . Details on 2D maps as in Fig. 1.

TABLE 1. Influence of receptive-field eccentricity on some basic visual characteristics of V6A neurons

	Orientation selective cells	Direction selective cells	Cells sensitive to complex visual stimuli	Cells sensitive only to slow motion
Centre	43/73 (59%)	38/57 (67%)	74/203 (36%)	24/69 (35%)
Periphery	53/103 (51%)	59/93 (63%)	54/329 (16%)	14/122 (11%)
Chi-square test	$P = 0.33$	$P = 0.69$	$P < 0.0001$	$P = 0.0001$

Centre: visual cells with receptive-field centres within 20° from the fovea. Periphery: visual cells with receptive-field centres more eccentric than 20° . Criteria used to classify the cells are as follows: orientation selective cell, unresponsive to stimulus orientation at 45° with respect to the preferred one; direction selective cell, unresponsive to a correctly orientated stimulus moving in the direction opposite to the preferred one; cell sensitive to complex visual stimuli, see description in the Materials and methods section; cell sensitive only to slow motion, responsive only to speeds of stimulus movement $<10^\circ/s$.

are reported. Neither quadrants nor hemifields are predominantly represented in different parts of V6A. The absence of upper-field representations in the ventrolateral part of V6A and of ipsilateral representations in the most medial part of V6A could be not significant, as both fields are underrepresented in V6A and their absence might be due to a recording bias. More data are needed to settle this question.

A different splitting of the visual field was also tested: centre vs. periphery, instead of quadrants, or hemifields. The upper part of Fig. 8 shows an example of this study in the same case reported in Fig. 7. Data reported in Fig. 8 show again the breakdown of retinotopic representation of the visual field in V6A, as both centre and periphery are represented in many parts of the area. However, the central representation is predominantly represented dorsally whereas the far periphery is almost

exclusively represented ventrally, near the border with area V6. This behaviour has been consistently observed in all the hemispheres we studied and is clearly recognizable also in the summary map shown in the lower part of Fig. 8. This dorso/ventral asymmetry is the only reliable sign of retinotopic organization in V6A.

In the view that cells with receptive field centrally or peripherally located could analyse different visual information, we searched for the existence of relationships between basic visual characteristics and receptive-field eccentricity in V6A neurons. To do this, visual neurons were divided in two samples: cells with a receptive-field centre inside the central 20° of the visual field and cells with a receptive field more eccentric than 20° . The choice of 20° as a discriminant value between the two samples was due to the fact that 20° was the mean size of foveal

receptive fields in V6A (see Fig. 3). As reported in Table 1, this analysis showed that the percentages of cells selective for orientation and direction of movement, although highly represented in V6A, were not significantly different in central vs. peripheral samples. On the contrary, cells activated only by complex visual stimuli and cells sensitive only to very slow speeds of movement (below $10^\circ/s$; most of them (17 of 24) well responsive also to stationary stimuli) were much more represented in the central sample than in the peripheral one.

Discussion

In a previous paper we described the functional and anatomical tools to recognize the cortical visual areas V6 and V6A in the APO in macaque monkey (Galletti *et al.*, 1996). The present work describes brain location, extent and visuotopic organization of one of them, area V6A.

Figure 9 shows the brain location and extent of area V6A. The dorsal and ventral borders of V6A shown in the figure can be considered as reliable, as we have also recorded from neurons outside area V6A, in areas PEc dorsally and V6 ventrally. On the contrary, the medial and lateral borders of area V6A might actually extend more anteriorly than shown in Fig. 9, as there we have not recorded from cells outside area V6A.

Laterally, area V6A adjoins the medial wall of IPs, where a visual area (area MIP) has been described to occupy the middle third of the caudal half of the wall (Colby *et al.*, 1988). In vertical penetrations passing through this cortical region, Colby & Duhamel (1991) found first a purely somatosensory region, then a region with bimodal (somatosensory and visual) neurons, and finally a purely visual region. There is clearly a similarity between the dorso/ventral somatosensory-to-visual gradient observed in the medial wall of IPs and the same dorso/ventral gradient we observed in APO, from PEc dorsally, to V6A and then V6 ventrally. Therefore, it could be argued that V6A and V6 are the extension in APO of the bimodal and purely visual regions, respectively, observed in the caudal half of the medial wall of IPs. However, a number of reasons tend to discard this possibility. First, in the intraparietal bimodal region almost all cells are bimodal in nature (Colby & Duhamel, 1991), whereas only a few are so in V6A (C. Galletti, unpublished observations). Second, cells in the bimodal region of the caudal intraparietal cortex are sensitive to visual stimuli but insensitive to the direction of movement of these stimuli (Colby & Duhamel, 1991), whereas about 70% of V6A cells are sensitive to the direction of movement of visual stimuli (Galletti *et al.*, 1996). Third, no cell modulated by oculomotor activity has been described in the medial bank of IPs, whereas more than half of V6A neurons are sensitive to oculomotor activity (Galletti *et al.*, 1991, 1995). Fourth, all the cells of the purely visual region of the caudal half of the medial wall of IPs are insensitive to the direction of movement of visual stimuli (Colby & Duhamel, 1991), whereas about 70% of cells in area V6 are direction-sensitive (Galletti *et al.*, 1996). There are enough reasons, we believe, to consider area V6A (and V6) as distinct visual areas with respect to those described in the medial wall of IPs.

Medially, area V6A adjoins area PGm (Pandya & Seltzer, 1982), on the medial surface of the hemisphere. A recent study has reported that the cells in area PGm are insensitive to pure visual stimuli (Ferraina *et al.*, 1997). In contrast, about 60% of the cells we have recorded from the medial surface of the hemisphere were sensitive to visual stimulation. In addition, the non-visual neurons we have recorded from the medial surface of the hemisphere had the same functional characteristics we observed in APO. In summary, we have no reason to believe that we recorded from cells outside area V6A when recording from the medial surface of the hemisphere. We believe that the medial part of

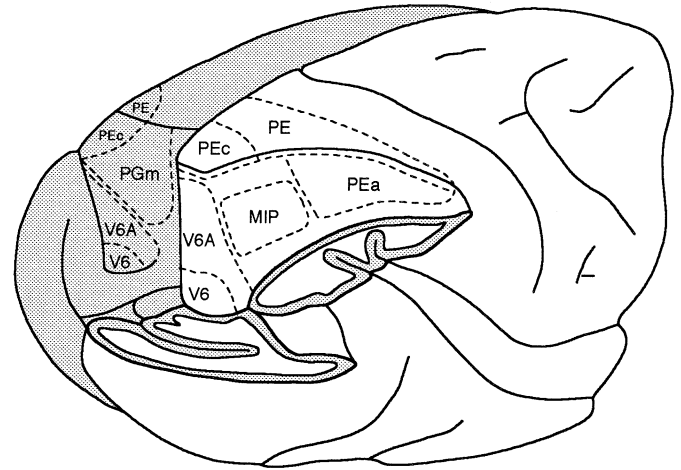


FIG. 9. Brain location and extent of area V6A. Posterolateral view of a partially dissected right hemisphere (grey matter in grey) and of the medial surface of left hemisphere (in grey) in macaca brain. The inferior parietal lobule of the right hemisphere has been cut away at the level of the fundus of IPs to show the cortex of the medial bank of this sulcus. The occipital lobe of the same hemisphere has been cut away at the level of the fundus of parieto-occipital and lunate sulci to show the cortex of the anterior bank of parieto-occipital sulcus. Location and extent of areas PE, PEa, PEc and PGm are according to Pandya & Seltzer (1982); area MIP is according to Colby *et al.* (1988); areas V6 and V6A are according to present results.

V6A occupies the caudalmost part of the medial surface of SPL, just behind area PGm, as indicated in Fig. 9.

Functional organization of area V6A

A number of reasons suggest that area V6A is involved in the control of reaching out and grasping objects. Reaching out a hand for an object is a multistage process, with an initial 'ballistic' movement of the hand towards the egocentric region of space where the object is located, followed by shaping of the hand according to the object features, and by corrective adjustments to exactly match hand location and shaping with location and features of the object (e.g. Jeannerod, 1988). It is evident that this multistage process needs visual information by both central and peripheral parts of the visual field, and V6A can provide these information. The neural control of this multistage process needs neuronal networks whose cells are sensitive to the direction of movement of visual objects. V6A neurons are able to code these information. Direction-selective cells, present in high percentage in area V6A (Galletti *et al.*, 1996), might participate in visual monitoring of the moving limb during prehension. They could signal the direction of arm movement when it passes through their receptive fields while moving towards the target of reaching. Cells sensitive only to very slow speeds of movement, many of them direction-selective as well, with a central receptive field and well responsive to stationary stimuli, could be engaged in the control of the final steps of reaching movement, when the hand approaches its target. To this regard, it is noteworthy that area V6A has a large representation of the central part of the visual field, where this control process is more effective.

Present results show that the upper visual field is less represented than the lower one in V6A. As area V6A is non-retinotopically organized, it seems hard to believe that this under-representation is due to a recording bias. On the other hand, overrepresentation and smaller receptive-field size in the lower visual field both agree with the view of a role for V6A in visual guiding of reaching. As a matter of fact, when the arms move towards visual targets they almost exclusively pass through the lower visual field of the subject. In particular, they pass through the medial part of the lower visual field, the most represented one in V6A (see Fig. 4).

To grasp an object, it is necessary to know its location in space. Everybody can reach out the location of visual targets without visual feedback and independently of the location of target image on the retinas (i.e. independent of the position of the eye, head or body). To allow this, one can suppose that the motor system controlling prehension uses representations of visual stimuli mapped in body-centred coordinates rather than retinal coordinates. In area V6A, these coordinates are directly encoded by real-position cells (Galletti *et al.*, 1993). As recently suggested by Galletti *et al.* (1995), the real-position behaviour could be the result of inputs coming from gaze-dependent visual cells whose receptive fields are in completely different parts of the visual field. In this view, the large scattering of visual receptive fields observed in V6A could be useful to build-up the real-position behaviour in local networks. Note that in V6A a large part of the visual field is repeatedly represented in small cortical regions (see penetrations a, b, c in Fig. 6A and f, g, h in Fig. 6B). Each one of these restricted cortical regions could be a local network devoted to building up the real-position behaviour.

We suggested (Galletti *et al.*, 1993, 1995, 1996) that the real-position cells send information about the spatial coordinates of visual objects to the dorsal frontal cortex, where premotor arm movement-related neurons were described (Caminiti *et al.*, 1991). Recent data confirm the presence of direct, strong connection between V6A and dorsal frontal cortex (Matelli *et al.*, 1995; Shipp & Zeki, 1995). Premotor neurons in dorsal area 6 could use real-position input to direct the initial, 'ballistic' movement of reaching action towards the target of reaching. In turn, premotor frontal neurons could send an efference copy of the motor command back to area V6A, as suggested by the presence of arm movement-related neurons in V6A (Galletti *et al.*, 1997a), for matching the willingness and effectiveness of the motor act. In agreement with this view, patients with damage in the caudal pole of SPL are unable to reach out for objects present in their visual field (Perenin & Vighetto, 1988). They did not show pure motor deficits. Patients are unable to pick-up a cup of coffee from the table and have great difficulty in placing it back, but have no problem in bringing the cup to the mouth and drink the coffee if someone put it in their hands (McCarthy & Warrington, 1990). It has been clearly demonstrated that these patients are impaired in directing the hand towards a visual target when a ballistic movement is required (Ratcliff & Davies-Jones, 1972). In other words, although they see the target, they are not able to use information about its spatial location to direct hand movement.

As previously mentioned, the knowledge of object spatial location is not enough to grasp it; it is also necessary to know its size, form and orientation in space, in order to adapt grip aperture and hand orientation to the visual features of the object to be reached out. Many V6A neurons are very sensitive to the orientation of stationary visual stimuli (Galletti *et al.*, 1996), and most of the cells sensitive to complex shapes have receptive fields in the central part of the visual field. Area V6A could thus provide critical visual information to the motor structures controlling orientation of the hand during arm-reaching movements. The fibres directly connecting V6A with dorsal frontal cortex besides conveying the spatial coordinates of the target of reaching could convey also this type of information, and this could explain why patients with damage in the caudal pole of SPL are not only impaired in directing arm-reaching movements, but also in orienting the hand according to the object features (Perenin & Vighetto, 1988).

Acknowledgements

The authors wish to thank L. Sabatini and G. Mancinelli for mechanical and electronic assistance, S. Boninsegna for technical assistance during experiments, and Chemical Industries Bracco S.p.A. for supplying the neurosurgical cement

(Refobacin-Palacos R, Merck, Germany). This work was supported by Grants from Ministero dell'Università e della Ricerca Scientifica e Tecnologica and Consiglio Nazionale delle Ricerche, Italy.

Abbreviations

ANCOVA, analysis of covariance; APO, anterior bank of parieto-occipital sulcus; IPL, inferior parietal lobule; IPs, intraparietal sulcus; MIP, medial intraparietal area; PEc, caudal PE area; PGm, medial PG area; PO, parieto-occipital area; SPL, superior parietal lobule.

References

- Bach, M., Bouis, D. & Fischer, B. (1983) An accurate and linear infrared oculometer. *J. Neurosci. Methods*, **9**, 9–14.
- Brodman, K. (1909) *Vergleichende Localisationslehre der Grosshirnrinde in Ihren Prinzipien Dargestellt auf Grund des Zellenbaues*. Barth, Leipzig.
- Caminiti, R., Johnson, P.B., Galli, C., Ferraina, S. & Burnod, Y. (1991) Making arm movements within different parts of space: the premotor and motor cortical representation of a coordinate system for reaching to visual targets. *J. Neurosci.*, **11**, 1182–1197.
- Colby, C.L. & Duhamel, J.R. (1991) Heterogeneity of extrastriate visual areas and multiple parietal areas in the macaque monkey. *Neuropsychologia*, **29**, 517–537.
- Colby, C.L., Gattass, R., Olson, C.R. & Gross, C.G. (1988) Topographical organization of cortical afferents to extrastriate visual area PO in the macaque: A dual tracer study. *J. Comp. Neurol.*, **269**, 392–413.
- Ferraina, S., Garasto, M.R., Battaglia-Mayer, A., Ferraresi, P., Johnson, P.B., Laquaniti, F. & Caminiti, R. (1997) Visual control of hand-reaching movement: activity in parietal area 7m. *Eur. J. Neurosci.*, **9**, 1090–1095.
- Galletti, C., Battaglini, P.P. & Fattori, P. (1991) Functional properties of neurons in the anterior bank of the parieto-occipital sulcus of the macaque monkey. *Eur. J. Neurosci.*, **3**, 452–461.
- Galletti, C., Battaglini, P.P. & Fattori, P. (1993) Parietal neurons encoding spatial locations in craniotopic coordinates. *Exp. Brain Res.*, **96**, 221–229.
- Galletti, C., Battaglini, P.P. & Fattori, P. (1995) Eye position influence on the parieto-occipital area PO (V6) of the macaque monkey. *Eur. J. Neurosci.*, **7**, 2486–2501.
- Galletti, C., Fattori, P., Battaglini, P.P., Shipp, S. & Zeki, S. (1996) Functional demarcation of a border between areas V6 and V6A in the superior parietal gyrus of the macaque monkey. *Eur. J. Neurosci.*, **8**, 30–52.
- Galletti, C., Fattori, P., Kutz, D.F. & Battaglini, P.P. (1997a) Arm movement-related neurons in the visual area V6A of the macaque superior parietal lobule. *Eur. J. Neurosci.*, **9**, 410–414.
- Galletti, C., Fattori, P., Kutz, D.F. & Gamberini, M. (1997b) Visual topography and cortical distribution of non-visual activities in area V6A of macaque superior parietal lobule. *Soc. Neurosci. Abstr.*, **23**, 604.13.
- Jeannerod, M. (1988) *The neural and behavioural organization of goal-directed movements*. Oxford University Press, Oxford.
- Matelli, M., Luppino, G., D'Amelio, M., Fattori, P. & Galletti, C. (1995) Frontal projections of a visual area (V6A) of the superior parietal lobule in macaque monkey. *Soc. Neurosci. Abstr.*, **21**, 169.8.
- McCarthy, R. & Warrington, E.K. (1990) *Cognitive Neuropsychology, a Clinical Introduction*. Academic Press, San Diego.
- Pandya, D.N. & Seltzer, B. (1982) Intrinsic connections and architectonics of posterior parietal cortex in the rhesus monkey. *J. Comp. Neurol.*, **204**, 196–210.
- Perenin, M.T. & Vighetto, A. (1988) Optic ataxia: a specific disruption in visuomotor mechanisms. I. Different aspects of the deficit in reaching for objects. *Brain*, **111**, 643–674.
- Ratcliff, G. & Davies-Jones, G.A.B. (1972) Defective visual localization in focal brain wounds. *Brain*, **95**, 49–60.
- Shipp, S. & Zeki, S. (1995) Direct visual input to premotor cortex from superior parietal cortex (areas V6 and V6A) in the macaque monkey. *Eur. J. Neurosci.*, **7** (Suppl. 8), 32.24.
- Stein, J.F. (1991) Space and the parietal association areas. In Paillard, J. (ed), *Brain and Space*. Oxford University Press, Oxford, pp. 185–222.
- Suzuki, H. & Azuma, M. (1976) A glass-insulated 'elgiloy' microelectrode for recording unit activity in chronic monkey experiments. *Electroencephalogr. Clin. Neurophysiol.*, **41**, 93–95.
- Van Essen, D.C. & Zeki, S.M. (1978) The topographic organization of rhesus monkey prestriate cortex. *J. Physiol. (London)*, **277**, 193–226.
- Von Bonin, G. & Bailey, P. (1947) *The Neocortex of Macaca mulatta*. University of Illinois Press, Urbana.